Use this document as a template

# My PhD Thesis

**Customise this page according to your needs**

Tobias Hangleiter[*]

March 31, 2025

[*] A LaTeX lover/hater

The kaobook class

The harmony of the world is made manifest in Form and Number, and the heart and soul and all the poetry of Natural Philosophy are embodied in the concept of mathematical beauty.

– D'Arcy Wentworth Thompson

# Contents

# A Flexible Python Tool For Fourier-Transform Noise Spectroscopy

# Introduction | 1

Noise is ubiquitous in condensed matter physics experiments, and in mesoscopic systems in particular it can easily drown out the sought-after signal. Hence, characterizing (and subsequently mitigating) noise is an essential task for the experimentalist. But noise comes in as many different forms as there are types of signal sources and detectors, whether it be a voltage source or a photodetector, and while some instruments have built-in solutions for noise analysis, they vary in functionality and capability. Moreover, the measured signal often does not directly correspond to the noisy physical quantity of interest, making it desirable to be able to manipulate the raw data before processing.

There exists a multitude of methods for estimating noise properties.

If the noisy process $x(t)$[1] has Gaussian statistics, meaning that the value at a given point in time follows a normal distribution with some mean $\mu$ and variance $\sigma^2$ over multiple realizations of the process, it can be fully described by the power spectral density (PSD) $S(\omega)$.[2] For the purpose of noise estimation, the assumption of Gaussianity is a rather weak one as the noise typically arises from a large ensemble of individual fluctuators and is therefore well approximated by a Gaussian distribution by the central limit theorem.[3] Even if the process $x(t)$ is not perfectly Gaussian, non-Gaussian contributions can be seen as higher-order contributions if viewed from the perspective of perturbation theory, and therefore the PSD still captures a significant part of the statistical properties. For this reason, the PSD is the central quantity of interest in noise spectroscopy and I will discuss some of its properties in the following.

For real signals $x(t) \in \mathbb{R}$, $S(\omega)$ is an even function and one therefore distinguishes the *two-sided* PSD $S^{(2)}(\omega)$ defined over $\mathbb{R}$ from the *one-sided* PSD $S^{(1)}(\omega) = 2S^{(2)}(\omega)$ defined only over $\mathbb{R}^+$. Complex signals $x(t) \in \mathbb{C}$ such as those generated by Lock-in amplifiers after demodulation in turn have asymmetric, two-sided PSDs.

## 2.1 Spectrum estimation from time series

To see how the PSD may be estimated from time-series data, consider a continuous wide-sense stationary[4] signal in the time domain $x(t) \in \mathbb{C}$ that is observed for some time $T$. We define the windowed Fourier transform of $x(t)$ and its inverse by[5]

$$\hat{x}_T(\omega) = \int_0^T \mathrm{d}t\, x(t) \mathrm{e}^{-\mathrm{i}\omega t} \tag{2.1}$$

$$\text{and} \quad x(t) = \int_{-\infty}^{\infty} \frac{\mathrm{d}\omega}{2\pi} \hat{x}_T(\omega) \mathrm{e}^{\mathrm{i}\omega t}, \tag{2.2}$$

*i.e.*, we assume that outside of the window of observation $x(t)$ is zero. The auto-correlation function of $x(t)$ is given by

$$C(\tau) = \langle x(t)^* x(t+\tau) \rangle \tag{2.3}$$

$$= \lim_{T \to \infty} \frac{1}{T} \int_0^T \mathrm{d}t\, x(t)^* x(t+\tau), \tag{2.4}$$

where $\langle \cdot \rangle$ is the ensemble average over multiple realizations of the process and the last equality holds true for ergodic processes. Expressing $x(t)$ in terms of its Fourier representation (Equation 2.1) and reordering the integrals, we get[6]

---

1: We discuss only classical noise here, meaning $x(t)$ commutes with itself at all times. For descriptions of and spectroscopy protocols for quantum noise refer to Refs. 1 and 2, for example.

2: The term *power spectrum* is often used interchangably. I will do so as well, but emphasize at this point that in digital signal processing in particular, the *spectrum* is a different quantity from the *spectral density*.

3: As an example, consider electronic devices, where voltage noise arises from a large number of defects and other charge traps in oxides being populated and depopulated at certain rates $\gamma$. The ensemble average over these so-called two-level fluctuators (TLFs) then yields the well-known $1/f$-like noise spectra (at least for a large density [3]).

4: For a wide-sense stationary (also called weakly stationary) process $x(t)$, the mean is constant and the auto-correlation function $C(t,t') = \langle x(t)^* x(t') \rangle$ is given by $\langle x(t)^* x(t+\tau) \rangle = \langle x(0)^* x(\tau) \rangle$ with $\tau = t' - t$. That is, it is a function of only the time lag $\tau$ and not the absolute point in time. For Gaussian processes as discussed here, this also implies stationarity [4]. The property further implies that $C(\tau)$ is an even function.

5: In this chapter we will always denote the Fourier transform of some quantity $\xi$ using the same symbol with a hat, $\hat{\xi}$.

6: Mathematicians might at this point argue the integrability of $x(t)$, but as we deal with physical processes with finite bandwidth (and have no shame), we do not.

$$C(\tau) = \lim_{T\to\infty} \frac{1}{T} \int_0^T dt \int_{-\infty}^\infty \frac{d\omega}{2\pi} \hat{x}_T(\omega)^* e^{-i\omega t} \int_{-\infty}^\infty \frac{d\omega'}{2\pi} \hat{x}_T(\omega') e^{i\omega'(t+\tau)} \quad (2.5)$$

$$= \lim_{T\to\infty} \frac{1}{T} \int_{-\infty}^\infty \frac{d\omega}{2\pi} \int_{-\infty}^\infty \frac{d\omega'}{2\pi} \hat{x}_T(\omega)^* \hat{x}_T(\omega') e^{i\omega'\tau} \int_0^T dt\, e^{it(\omega'-\omega)} \quad (2.6)$$

The innermost integral approaches a $\delta$-function for large $T$,[7] allowing us to further simplify this under the limit as

$$C(\tau) = \lim_{T\to\infty} \frac{1}{T} \int_{-\infty}^\infty \frac{d\omega}{2\pi} \int_{-\infty}^\infty \frac{d\omega'}{2\pi} \hat{x}_T(\omega)^* \hat{x}_T(\omega') e^{i\omega'\tau} \delta(\omega'-\omega) \quad (2.7)$$

$$= \lim_{T\to\infty} \frac{1}{T} \int_{-\infty}^\infty \frac{d\omega}{2\pi} |\hat{x}_T(\omega)|^2 e^{i\omega\tau} \quad (2.8)$$

$$= \int_{-\infty}^\infty \frac{d\omega}{2\pi} S(\omega) e^{i\omega\tau} \quad (2.9)$$

with the PSD

$$S(\omega) = \lim_{T\to\infty} \frac{1}{T} |\hat{x}_T(\omega)|^2 \quad (2.10)$$

$$= \int_{-\infty}^\infty d\tau\, C(\tau) e^{-i\omega\tau} \quad (2.11)$$

Equation 2.9 is the Wiener-Khinchin theorem that states that the auto-correlation function $C(\tau)$ and the PSD $S(\omega)$ are Fourier-transform pairs [4]. Furthermore, defining the latter through Equation 2.10 gives us an intuitive picture of the PSD if we recall Parseval's theorem,

$$\int_{-\infty}^\infty \frac{d\omega}{2\pi} \frac{1}{T} |\hat{x}_T(\omega)|^2 = \frac{1}{T} \int_{-\infty}^\infty dt\, |x(t)|^2. \quad (2.12)$$

That is, the total power $P$ contained in the signal $x(t)$ is given by integrating over the PSD. Similarly, the power contained in a band of frequencies $[\omega_1, \omega_2]$ is given by

$$P(\omega_1, \omega_2) = \mathrm{rms}\,(\omega_1, \omega_2)^2 \quad (2.13)$$

$$= \int_{\omega_1}^{\omega_2} \frac{d\omega}{2\pi} S(\omega) \quad (2.14)$$

where $\mathrm{rms}\,(\omega_1, \omega_2)$ is the root-mean-square within this frequency band. These relations are helpful when analyzing noise PSDs to gauge the relative weight of contributions from different frequency bands to the total noise power.

ref

Equation 2.10 represents the starting point for the experimental spectrum estimation procedure. Instead of a continuous signal $x(t), t \in [0, T]$, consider its discretized version[8]

$$x_n, \quad n \in \{0, 1, \ldots, N-1\} \quad (2.15)$$

defined at times $t_n = n\Delta t$ with $T = N\Delta t$ and where $\Delta t = f_s^{-1}$ is the sampling interval (the inverse of the sampling frequency $f_s$). Invoking the ergodic theorem, we can replace the long-term average in Equation 2.10 by the ensemble average over $M$ realizations $i$ of the noisy signal $x_n^{(m)}$

and write

$$S_n = \frac{1}{M} \sum_{i=0}^{M-1} \left| \hat{x}_n^{(m)} \right|^2 \qquad (2.16)$$

$$= \frac{1}{M} \sum_{i=0}^{M-1} S_n^{(m)} \qquad (2.17)$$

where $\hat{x}_n^{(m)}$ is the discrete Fourier transform of $x_n^{(m)}$, we defined the *periodogram* of $x_n^{(m)}$ by

$$S_n^{(m)} = \left| \hat{x}_n^{(m)} \right|^2, \qquad (2.18)$$

and $S_n$ is an *estimate* of the true PSD sampled at the discrete frequencies $\omega_n = 2\pi n/T \in 2\pi \times \{-f_s/2, \dots, f_s/2\}$.[9] Equation 2.16 is known as Bartlett's method [5] for spectrum estimation.[10]

To better understand the properties of this estimate, let us take a look at the parameters $\Delta t$, $N$, and $M$. The sampling interval $\Delta t$ defines the largest resolvable frequency by the Nyquist sampling theorem,

$$f_{\max} = \frac{f_s}{2} = \frac{1}{2\Delta t}. \qquad (2.19)$$

In turn, the number of samples $N$ determines the frequency resolution $\Delta f$, or smallest resolvable frequency,

$$f_{\min} = \Delta f = \frac{1}{T} = \frac{1}{N\Delta t} = \frac{f_s}{N}. \qquad (2.20)$$

Lastly, $M$ determines the variance of the set of periodograms $\{S_n^{(m)}\}_{i=0}^{M-1}$ and hence the accuracy of the estimate $S_n$.

In practice, the ensemble realizations $i$ are of course obtained sequentially, implying that one acquires a time series of data $x_n, n \in \{0, 1, \dots, NM-1\}$ and partitions these data into $M$ sequences of length $N$. It becomes clear, then, that the Bartlett average (Equation 2.16) trades spectral resolution (larger $N$) for estimation accuracy (larger $M$) given the finite acquisition time $T = NM\Delta t$.

An improvement in data efficiency can be obtained using Welch's method [6]. To see how, we first need to discuss spectral windowing.

## 2.2 Window functions

Partitioning a signal $x_n$ into $M$ sections $x_n^{(m)}$ of length $N$ is mathematically equivalent to multiplying the signal with the rectangular *window function* given by[11]

$$w_n^{(m)} = \begin{cases} 1 & \text{if} \quad (m-1)N \le n < mN \quad \text{and} \\ 0 & \text{else} \end{cases} \qquad (2.21)$$

so that $x_n^{(m)} = x_n w_n^{(m)}$.

9: We blithely disregard integer algebra issues occuring here for conciseness and leave it as an exercise for the reader to figure out what the exact bounds of the set of $\omega_n$ are.
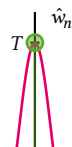
10: By taking the limit $M \to \infty$ one recovers the true PSD,

$$\lim_{M\to\infty} S_n = S(\omega_n).$$

The continuum limit is as always obtained by sending $\Delta t \to 0, N \to \infty, N\Delta t = $ const.

11: This window is also known as the boxcar or Dirichlet window.

add $\omega_n^{(m)}$, scaled ticks

$\hat{w}_n$

$T$

Now recall that multiplication and convolution are duals under the Fourier transform, implying that

$$\hat{x}_n^{(m)} = \hat{x}_n * \hat{w}_n^{(m)}. \tag{2.22}$$

where the Fourier representation of the rectangular window[12]

$$\hat{w}_n^{(m)} = \hat{w}_n e^{-i(m-1/2)\omega_n T}, \tag{2.23}$$

$$\hat{w}_n = T \operatorname{sinc}\left(\frac{\omega_n T}{2}\right). \tag{2.24}$$

Figure 2.1 shows the unshifted rectangular window $\hat{w}_n$ in Fourier space. We can hence understand the Fourier spectrum of $x_n^{(m)}$ as sampling $\hat{x}_n$ with the probe $\hat{w}_n^{(m)}$. However, while in the continuum limit (c.f. sidenote 10) Equation 2.24 tends towards $\delta(\omega_n)$ and thus will produce a faithful reconstruction of the true spectrum, the finite frequency spacing $\Delta f$ of discrete signals introduces a finite bandwidth of the probe as well as *sidelobes*. These effects induce what is known as *spectral leakage* [4, 7] and lead to artifacts and deviations of the spectrum estimator $S_n$ from the true spectrum $S(\omega_n)$.

For this reason, a plethora of *window functions* have been introduced to mitigate the effects of spectral leakage. Key properties of a window are the spectral bandwidth (center lobe width) and sidelobe amplitude between which there typically is a tradeoff.[13]

13: Wikipedia gives a good overview of existing window functions [8].
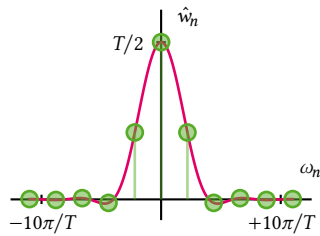
add $\omega_n^{(m)}$, scaled ticks



**Figure 2.2:** The Fourier representation of the Hann window in continuous time.

A window frequently used in spectral analysis is the Hann window [9],

$$w_n^{(m)} = \begin{cases} \cos^2\left(\frac{\pi n}{N}\right) & \text{if} \quad (m-1)N \le n < mN \quad \text{and} \\ 0 & \text{else} \end{cases} \tag{2.25}$$

with the Fourier representation of the unshifted window,

$$\hat{w}_n = T \operatorname{sinc}\left(\frac{\omega_n T}{2}\right) \times \frac{1}{2(1 - \omega_n T/2\pi)(1 + \omega_n T/2\pi)}, \tag{2.26}$$

shown in Figure 2.2. The favorable properties of the Hann window are apparent when compared to the rectangular window in Figure 2.1; the sidelobes are quadratically suppressed while the center lobe is only slightly broadened.

Another favorable property of the Hann window is that $w_0^{(0)} = w_{N-1}^{(0)} = 0$. This suppresses detrimental effects arising from a possible discontinuity $(x_0^{(0)} \ne x_{N-1}^{(0)})$ at the edge of a data segment related to the discrete Fourier transform, which assumes periodic data.[14]

14: Although this can usually also be achieved by detrending the data before performing the Fourier transform, which is a good idea in any case.

## 2.3 Welch's method

Contemplating Equation 2.25, one might come to the conclusion that using a window such as this is not very data efficient in the sense that a large fraction of samples located at the edge of the window is strongly suppressed and hence does not contribute significantly to the spectrum estimate. To alleviate this lack of efficiency, one can introduce an overlap between adjacent data windows. That is, instead of partitioning the data

$x_n$ into $M$ non-overlapping sections of length $N$, one shifts the $m$th window forward by $-mK$ with $K > 0$ the overlap. Finally, the periodogram (Equation 2.18) is computed for each window and subsequently averaged to obtain the spectrum estimator (Equation 2.16).

This method of spectrum estimation is known as Welch's method [6]. One can show [6] that the correlation between the periodograms of adjacent, overlapping windows is sufficiently small to avoid a biased estimate. The overlap naturally depends on the choice of window; a typical value for the Hann window $K = N/2$ with which one would obtain $M = 2L/N - 1$ windows for data of length $L$.[15]
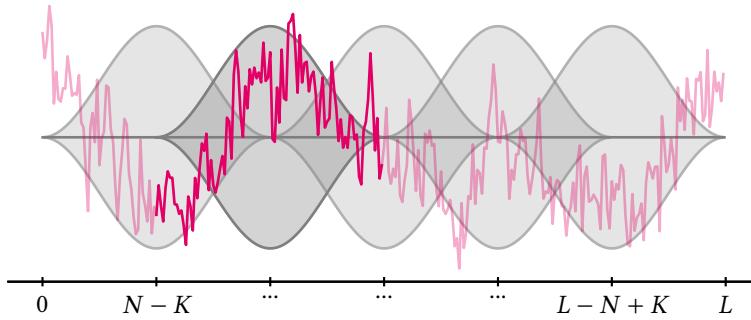
15: Again neglecting integer arithmetic issues.



**Figure 2.3:** Illustration of Welch's method for spectrum estimation. The data (pink) of length $L$ is partitioned into $K = 2L/N - 1$ segments of length $N$. Each segment is multiplied with a window function (gray) which reduces spectral leakage and other artifacts. A finite overlap $K$ between adjacent windows (gray) ensures efficient sample use.

Figure 2.3 conceptually illustrates Welch's method for a trace of $1/f$ noise with $L = 300$ samples in total. Choosing the Hann window and an overlap of 50 % results in $M = 5$ segments for a window length of $N = 100$. The data in the second window is highlighted.

## 2.3.1 Parameters

We are now in a position to discuss how the various parameters of a time series relate to both to physical parameters of the resulting spectrum estimate and to each other. To this end, we will go through the typical procedure of acquiring a spectrum estimate using Welch's method chronologically.

To acquire data using some form of (digital) data acquisition device (DAQ), one usually needs to specify two parameters first: the total number of samples to be acquired, $L$, and the sample rate, $f_s$. This results in a measurement of duration $T = L\Delta t$ where $\Delta t = f_s^{-1}$ as previously mentioned. The choice of $f_s$ already induces an upper bound on the first parameter characterizing the PSD estimate: the largest resolvable frequency $f_{max} \leq f_s/2$ (c.f. Equation 2.19, but note that we allow $f_{max}$ to be smaller than half the sample rate in anticipation of hardware constraints). Next, we choose a number of Welch averages, $M$, *i.e.*, data partitions, and their overlap, $K$. In doing so, one fixes the number of samples per partition $N$ and thereby induces the lower bound on the second parameter characterizing the PSD estimate: the frequency spacing $\Delta f = 1/N \leq f_{min}$ (c.f. Equation 2.20).[16]

**Table 2.1:** Overview of spectrum estimation parameters. The parameters can be assigned into three groups: 1. DAQ parameters configuring the data acquisition device, 2. Welch parameters specifying the periodogram averaging, and 3. Spectrum properties induced by the above.

| 1. DAQ parameters | |
| --- | --- |
| $L$ | Total number of samples |
| $f_s$ | Sample rate |
| **2. Welch parameters** | |
| $K$ | Number of overlap samples |
| $N$ | Number of segment samples |
| $M$ | Number of Welch segments |
| **3. Spectrum parameters** | |
| $f_{min}$ | Smallest resolvable frequency |
| $f_{max}$ | Largest resolvable frequency |

16: Technically, the smallest resolvable frequency in a fast Fourier transform (FFT) is zero, of course. But as data is typically detrended (a constant or linear trend subtracted) before computation of the periodogram, the smallest *meaningful* frequency is given by $f_{min}$.

D(A)G for parameter interdependencies?

# The `python_spectrometer` software package | 3

In this chapter, I will lay out the design and functionality of the `python_-spectrometer` Python package.

## 3.1 Package design and implementation

The `python_spectrometer` package provides a single user-facing class, `core.Spectrometer`, that manages the entire process from data acquisition to spectrum estimation and plotting. Plotting functionality is factored out into a private submodule for maintainability.

## 3.2 Feature overview

**Table 3.1:** Variable names used in Chapter 2 and their corresponding parameter names as used in `python_spectrometer` and `scipy.signal.welch()` [10].

| Variable | Parameter |
|---|---|
| $L$ | `n_pts` |
| $f_s$ | `fs` |
| $K$ | `noverlap` |
| $N$ | `nperseg` |
| $M$ | `n_seg` |
| $f_{min}$ | `f_min` |
| $f_{max}$ | `f_max` |

# Characterization and Improvements of a Millikelvin Confocal Microscope

# Electrostatic Trapping of Excitons in Semiconductor Membranes

# A Filter-Function Formalism For Quantum Operations

# APPENDIX

# Bibliography

[1]  A. A. Clerk et al. "Introduction to Quantum Noise, Measurement, and Amplification." In: *Rev. Mod. Phys.* 82.2 (Apr. 15, 2010), pp. 1155–1208. DOI: 10.1103/RevModPhys.82.1155. (Visited on 01/19/2022) (cited on page 5).

[2]  Gerardo A. Paz-Silva, Leigh M. Norris, and Lorenza Viola. "Multiqubit Spectroscopy of Gaussian Quantum Noise." In: *Physical Review A* 95.2 (Feb. 23, 2017), p. 022121. DOI: 10.1103/PhysRevA.95.022121 (cited on page 5).

[3]  M. Mehmandoost and V. V. Dobrovitski. "Decoherence Induced by a Sparse Bath of Two-Level Fluctuators: Peculiar Features of $1/F$ Noise in High-Quality Qubits." In: *Phys. Rev. Res.* 6.3 (Aug. 15, 2024), p. 033175. DOI: 10.1103/PhysRevResearch.6.033175. (Visited on 08/20/2024) (cited on page 5).

[4]  Lambert Herman Koopmans. *The Spectral Analysis of Time Series.* 2nd ed. Vol. 22. Probability and Mathematical Statistics. San Diego: Academic Press, 1995 (cited on pages 5, 6, 8).

[5]  M. S. Bartlett. "Smoothing Periodograms from Time-Series with Continuous Spectra." In: *Nature* 161.4096 (May 1948), pp. 686–687. DOI: 10.1038/161686a0. (Visited on 03/26/2025) (cited on page 7).

[6]  P. Welch. "The Use of Fast Fourier Transform for the Estimation of Power Spectra: A Method Based on Time Averaging over Short, Modified Periodograms." In: *IEEE Transactions on Audio and Electroacoustics* 15.2 (June 1967), pp. 70–73. DOI: 10.1109/TAU.1967.1161901 (cited on pages 7, 9).

[7]  F.J. Harris. "On the Use of Windows for Harmonic Analysis with the Discrete Fourier Transform." In: *Proceedings of the IEEE* 66.1 (Jan. 1978), pp. 51–83. DOI: 10.1109/PROC.1978.10837. (Visited on 03/27/2025) (cited on page 8).

[8]  *Window Function.* In: *Wikipedia.* Mar. 20, 2025. (Visited on 03/27/2025) (cited on page 8).

[9]  A. Nuttall. "Some Windows with Very Good Sidelobe Behavior." In: *IEEE Transactions on Acoustics, Speech, and Signal Processing* 29.1 (Feb. 1981), pp. 84–91. DOI: 10.1109/TASSP.1981.1163506. (Visited on 03/27/2025) (cited on page 8).

[10]  *Welch — SciPy v1.15.2 Manual.* URL: https://docs.scipy.org/doc/scipy/reference/generated/scipy.signal.welch.html (visited on 03/31/2025) (cited on page 11).

# Special Terms

**D**
**DAQ** data acquisition device. 9

**F**
**FFT** fast Fourier transform. 9

**P**
**PSD** power spectral density. 5–7, 9

**T**
**TLF** two-level fluctuator. 5